Indian J. Phys. 77A (6), 565-569 (2003)

AN INTERNATIONAL JOURNAL
IJPA

Fano resonances in presence of dephasing and evanescent modes

Colin Benjamin* and A M Jayannavar
Institute of Physics, Sachivalaya Marg, Bhubaneswar-751 005, Orissa, India
E-mail : colin@iopb.res.in

Abstract : In this work we analyze the effect of incoherent transport on Fano resonances. In close proximity to recent experimental results we find the transition from Fano to Lorentzian line-shapes with increasing incoherence. In the presence of evanescent wave propagation in the AB interferometer with a quantum well no Fano line shapes are observed. Only when one arm of the AB interferometer is made propagating do we recover Fano line-shapes.

Keywords : Dephasing, evanescent modes, Aharonov-Bohm rings, Fano resonances

PACS Nos. : 72.10 -d, 73.23.-b, 05.60 Gg, 85.35.Ds

1. Introduction

During the last two decades the subject of mesoscopic physics is being actively pursued. The interest ranges from fundamental physics to technological applications. Mesoscopic physics deals with samples whose sizes are intermediate between the atomic scale and the macroscopic scale determined by the phase-coherence length of the quasi-particles [1,2]. In these systems at low temperatures electrons are able to retain their phase coherence and hence exhibit quantum interference phenomena. These systems have revealed a new range of unexpected quantum phenomenon, often counter-intuitive [3]. Recently Fano resonances have been observed in a mesoscopic AB ring with a quantum dot embedded in it's upper arm [4]. Fano resonances arise when a discrete set of states are coupled to the continuum [5]. Especially Fano resonances are caused by interference of two alternative paths, a resonant and a non-resonant one. In the geometry considered a resonant path is *via* a quantum dot (having resonant energy levels) and a direct nonresonant path is via the lower arm of the ring (Figure 1).

Transmission resonances are generally of two types Breit-Wigner and Fano. The Breit-Wigner transmission line-shape is given by

$$T(E) = \frac{\Gamma^2}{(E-E)^2 + \frac{1}{4}\Gamma^2}$$

where E is the energy, E_r and Γ are the resonant energy and width respectively. The quantities E_r and Γ are related to the real and imaginary part of the pole of the scattering amplitude in the complex energy plane. Breit-Wigner line-shapes are symmetric. The form of a Fano line-shape Fano is given by

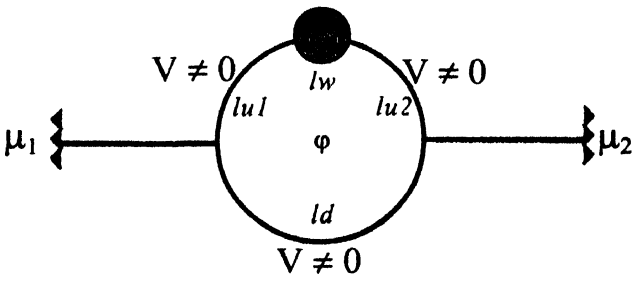

Figure 1. The Aharonov-Bohm ring wiht a quantum dot/quantum well in its upper arm.

*Corresponding Author

$$T(E) = Td\frac{|2E + q\Gamma|^2}{4E^2 + \Gamma^2}$$

In the above equations, $T = |t_d + t_r|^2$ is the transmission coefficient (conductance) with $t_d = e^{i\beta d}\sqrt{T_d}$ and $t_r(E) = z_r\Gamma/(2E + i\Gamma)$ describing the direct and resonant transmission amplitudes, E the energy, E_r and Γ the resonance anergy and width respectively. T_d the non-resonant conductance, and $q = i + z_r e^{-i\beta d}/\sqrt{G_d}$ the complex Fano parameter, see for details Ref. [6]. Note that Fano line-shapes are asymmetric as opposed to the symmetric Breit-Wigner line-shapes. They in contrast to Breit-Wigner forms have zero-pole pair structure in the complex energy plane of the scattering amplitude. It must be remembered that the above form of the Fano line-shape is obtained from scattering theory in the absence of dephasing. In mesoscopic devices these asymmetric structures in the conductance are seen as a function of a gate voltage or Fermi energy. The motivation of this work is to explain the transition of Fano to Lorentzian line-shapes in conductance with increasing temperature as seen in the recent experiment and also to analyze the need of propagating modes to observe suchline-shapes.

2. Effect of dephasing on Fano line-shapes

In an AB ring geometry as shown in Figure 1, if one embeds a quantum dot (QD) with a few bound states then because of the interplay between the bound states of QD and the continuum states of the open ring one gets Fano resonances. Our first interest in this work is to analyze the effect of dephasing on these Fano resonances. We formulate incoherence (or dephasing) using the method of wave attenuation. In this method, the particles are removed from the phase coherent channel and subsequently re-injected into the system so as to conserve the particle number. This leads to loss of phase memory and incoherence in the motion of quasi-particles. The proper method of re-injecting carriers as suggested by Brouwer and Beenakker [7] is followed which is in conformity with the fact that the two terminal conductance should be Onsager symmetric [8]. Moreover this method is a generalization of the voltage probe model [9] which has been successfully used in analyzing dephasing in mesoscopic systems. For this brief discussion we only write the formula for conductance used in plotting Figure 2.

$$G = T_2 + \frac{(1 - R_{11} - T_{21})(1 - R_{22} - T_{21})}{1 - R_{11} - T_{21} + 1 - R_{22} - T_{12}} \quad (1)$$

Here, G in demensionless form just denotes the total transmission in accordance with Landauer's formalism, which view conductance as transmission. All the above coefficients are built from the 2X2 S-matrix which represents the matrix of the non-hermitian or absorbing system. The first term in eq. (1) represents the conductance contribution from the phase coherent part. The second term accounts for electrons that are re-injected from the phase breaking reservoir, thereby ensuring particle conservation. This part also can be identified as a contribution to the conductance arising from the incoherent processes. The method of wave attenuation which means physically damping the wave with distance is dealt with elaborately in the ref. [8] and we have used this method to calculate the scattering co-efficients. In this method the wave attenuation factor α is identified as an incoherence parameter. Increasing temperature amounts to increasing incoherence and thus α. Therefore the parameter α which is inversely proportional to the inelastic mean free path can be obtained by fitting with experimental results. This method of wave attenuation has been used to model dephasing in AB ring interferometers [8], resonant tunneling diodes and to calculate the time taken by a particle to scatter (*i.e.* either reflect or transmit) from a region of space [10].

In the model, we consider a quantum dot placed on the upper arm of an open Aharonov-Bohm ring with a flux ϕ piercing the loop. The quantum dot has resonant discrete levels. We solve the problem using S-Matrix formulation [8]. The co-eficients of which are related to transmission and reflection amplitudes which are required to calculate the conductance eq. (1). The S-matrices of the three way junctions of the Aharonov-Bohm ring interferometer are parameterized by a single parameter ϵ which couples the leads to the AB interferometer. The form of the junction S-matrix is same as in Ref. [8]. We assume the discrete levels of the quantum dot to be having Breit-Wigner forms. Following the formalism of Sun and Lin [11], one can parameterize the pq^{th} element of the 2X2 S-Matrix of the quantum dot as-

$$S_{pq} = \delta_{pq} - \frac{i/2}{\sum_j \frac{\Gamma_j}{E - E_j} + i/2} \quad (2)$$

wherein Γ_j and E_j represent the width and energy of the j^{th} resonant level of the quantum dot while E denotes the

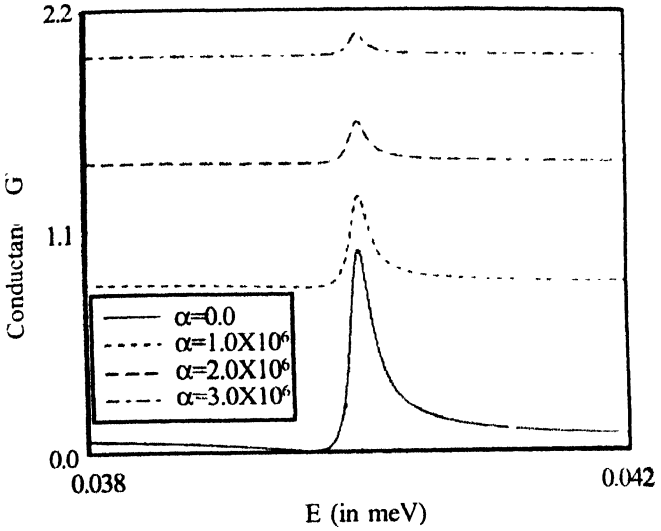

Figure 2. The conductance (G) *vs* E in meV. Quantum dot parameters (from eq. 2) are $E_1 = 0.04$, with $\Gamma_1 = 0.0001$. The conductance for increasing values of α in m^{-1} are shifted by 0.5 for clarity. The length parameters of the Aharnov-Bohm ring are $lu1 = lu2 = 5$Å, $ld = 10$Å. The coupling sterngth ϵ is 0.5 (maximal) and flux is 320 weber The ring as in the experiment is assumed to be of GaAs.

Fermi energy and p, q take on values 1 and 2. In our analysis we assume that the dot has single level at E_1. It should, however, be noted that unlike Sun and Lin, we neglect the intra-dot Coulomb interaction as in eq. (2). The quantum dot is placed symmetrically in the upper arm of the Aharonov-Bohm ring interferometer (Figure 1).

In Figure 2 we plot the conductance as a function of incident electron energy (in a narrow range) using eq. (1) for various values of incoherent parameter α. The physical parameters are as mentioned in the figure caption. In the absence of dephasing $\alpha = 0$ the line-shape is asymmetric and has a transmission zero. This is a perfect characterization of Fano resonance. As inelastic scattering parameter α is increased Fano line-shapes broaden and their peak values are reduced the zero in the conductance disappears. Subtracting the continuum background of the conductance, we see that the asymmetric Fano line-shapes evolve to symmetric line-shapes corresponding to Lorentzian or Breit-Wigner forms in similarity with experimental observations and also consistent with the treatment of Ref. [6]. The incoherence parameter 2α is defined as equal to inverse of the mean free path. A representative value of α in Figure 2, for example 1×10^6 corresponds to a mean free path of 5×10^7m which is in conformity with the millikelvin temperature range at which the experiment has been performed. The complete understanding requires details of physical parameters associated with the real experiment. The complex Fano parameter as defined above also changes with increase in dephasing strength, as seen in Ref. [6]. As the Fano resonance arises from interference of two transmission paths the line shape (Fano parameter q) is sensitive to dephasing and hence the dephasing time can be extracted from a measurement of q for a single Fano resonance alone.

3. Effect of evenecent modes on Fano line shapes

Next we focus on evansecent wave transport in the same AB ring interferometer set up as in Figure 1. The quantum dot is replaced by a quantum well (which has resonant levels) and the electron propagates as an evanescent wave throughout the ring but outside the well region. The ring is characterized by a potential V everywhere apart from the well which is at zero potential. The connecting leads are also set at zero potential. Thus when an electron with energy $E < V$ impinges on the ring it has to tunnel out of the ring. Only in the well and the connecting leads does the electron propagate with a real wave vector $k = \sqrt{E}$ elsewhere it propagates with a complex wave-vector $k = i\sqrt{V-E}$. In such situation the contribution to conductance arises simultaneously from two non-classical effects namely, Aharonov-Bohm effect and quantum tunelling [12]. Such situation can arise when the transverse width of the ring is much less than the connecting ideal wires. In this case due to the higher zero point energy arising from

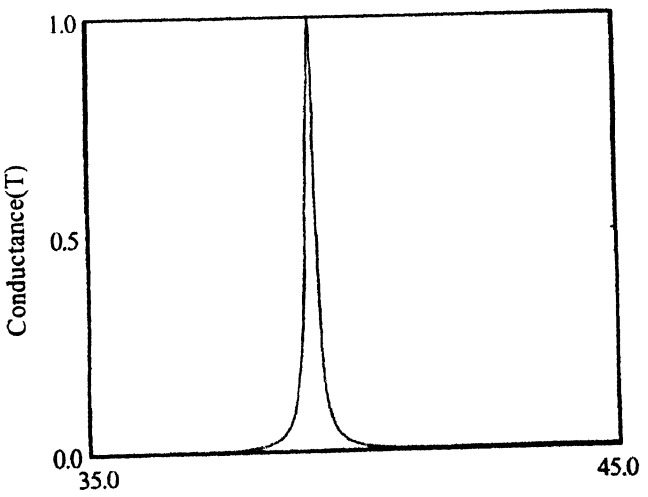

Figure 3. Evanescent transport for zero field and increasing energy. Barrier potential $V = 400.0$ and lengths are $lu1 = lu2 = 0.1$, $lw = 0.4$ and $ld = 0.4$ in demensionless units.

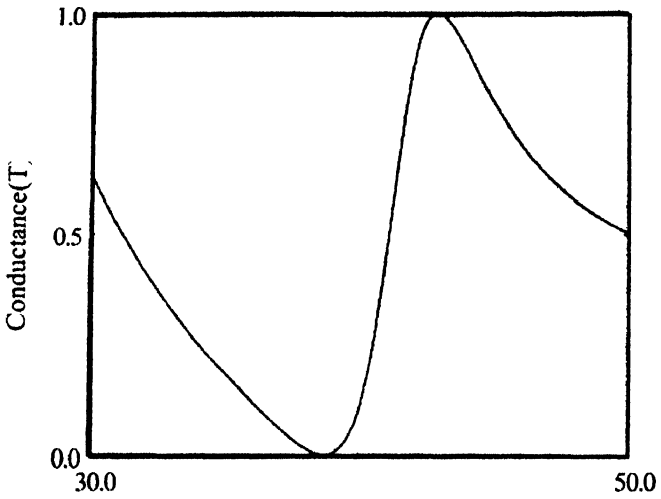

Figure 4. Fano resonant line-shapes. Lower arm is free (barrier absent). Same physical parameters as in Figure 3.

transverse confinement, the fundamental sub-band minima in the ring will be at higher energy than the value of few sub-band minima in the ideal connecting wires. Now a situation can arise where propagating modes in the wire have energy less than the minimum propagating sub-band energy of the ring system. Thus the electron propagating in a lower sub-band of the ideal wire feels a barrier to it's motion (experiences an effective potential barrier V, arising solely because of the mismatch of the zero-point energies) and tunnels across the system *via* evanescent mode propagation. For simplicity we have restricted our calculation to single channel case. We are interested only in coherent transport, *i.e.*, absence of dephasing. using the wave guide method [13,14] one can solve for all the scattering coefficients. In Figure 3 we plot the conductance (in effect the transmission coefficient in demensionless form) as function of the Femi energy across a small energy interval. All the physical parameters are in dimensionless units and are mentioned in the figure caption. We see resonant transport around the quasi bound states of the well. The line shape is that of Breit-Wigner form. We do not observe any Fano line-shapes as long as $E < V$. As mentioned earlier Fano line-shapes arise from the interference of two alternative paths, one resonant and another direct. Our results clearly indicate when the transport across the direct path is *via* evanescent modes, then Fano line-shapes are absent. To recover Fano line-shapes, direct path should be a propagating one. To see this explicitly we set potential in the lower arm to be zero. So that electron traverses the lower arm as a propagating wave. For this case, we have plotted in Figure 4, the conductance *versus* Fermi energy. We clearly see the Fano line-shapes around the same energy interval as in Figure 3, *i.e.*, line-shapes are asymmetric and transmission exhibits zero on the real axis. The results presented in Figures 3 and 4 are in the absence of magnetic field. Increasing the magnetic field which amounts to breaking the existing time reversal symmetry will lead to lifting of zeroes except when the flux piercing the loop is an intergral or half integral multiple of the flux quantum [15].

4. Conclusions

Our studies reveal that increasing incoherence causes asymmetric Fano line-shapes to evolve into the well known Breit-Wigner forms. When electron traverses as an evanescent wave in one of the alternative (non-resonant path) the system does not support Fano resonances. Transport in the presence of evanescent wave propagation exhibits other novel features as well. We have verified separately that the well known effect of current magnification [14] is absent for complete evanescent wave transport in the entire AB ring interferometer. Moreover magneto-conductance in this case as well as in the case discussed in Figure 3, exhibit a systematic behaviour robust against small perturbations. The application of these observations to quantum device (robust switch) [12] has been reported elsewhere.

References

[1] S Datta *Electron Transport in Mesoscopic Systems* (Cambridge : Cambridge University Press) (1995)

[2] Y Imry *An Introduction to Mesoscopic Physics* (Oxford : Oxford University Press) (2001)

[3] L I Glazman *Am. J. Phys.* **70** 376 (2002)

[4] K Kobayashi, H Aikawa, S Katsumoto and Y Iye *Phys. Rev. Lett.* **88** 256806 (2002)

[5] U Fano *Phys. Rev.* **124** 1866 (1961)

[6] A A Clerk, X Waintal and P W Brouwer *Phys. Rev. Lett.* **86** 4636 (2001)

[7] P W Brouwer and C W J Beenakker *Phys. Rev.* **B55** 4695 (1997); P W Brouwer Ph.D. thesis, Insttuut-Lorentz, University of Leiden, The Netherlands (1997)

[8] Colin Benjamin and A M Jayannavar *Phys. Rev.* **B65** 155309 (2002); Colin Benjamin and A M.Jayannavar preprint cond-mat/0209438

[9] M Büttiker *Phys. Rev.* **B33** 3020 (1986); *IBM J. Res. Dev.* **32** 63 (1988)

[10] C Benjamin and A M Jayannavar *Solid State Commun.* **121** 591 (2002)

[11] Q Sun and T Lin *Eur. Phys. J.* **B5** 913 (1998)

[12] P S Deo and A M Jayannavar *Mod. Phys Lett* **B8** 301 (1994); B C Gupta, P S Deo and A M Jayannavar *Int. J Mod Phys.* **B10** 3595 (1996)

[13] J B Xia *Phys. Rev.* **B45** 3593 (1992)

[14] P S Deo and A M Jayananvar *Phys Rev* **B50** 11629 (1994); T P Pareek, P S Deo and A M Jayananvar *Phys Rev.* **B52** 14657 (1995), Colin Benjamin and A M Jayannavar *Phys Rev* **B64** 233406 (2001)

[15] T Kim, S Y Cho, C K Kim and C M Ryu *Phys Rev* **B65** 245307 (2002)